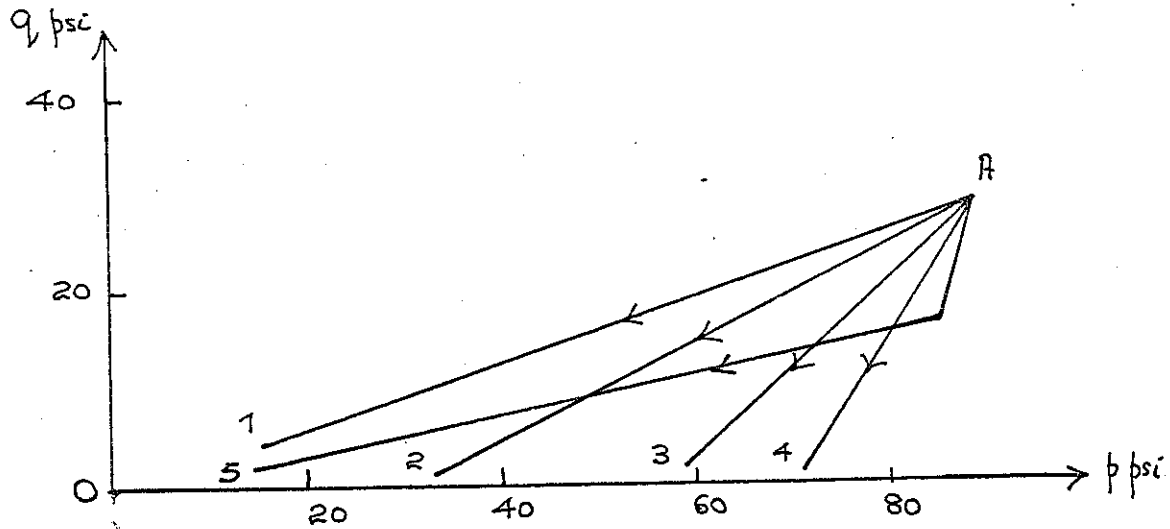


Fig. 7.40(a). Stress paths followed by specimen $T_{20}$ during unloading from a stress ratio of $\eta = 0.34$

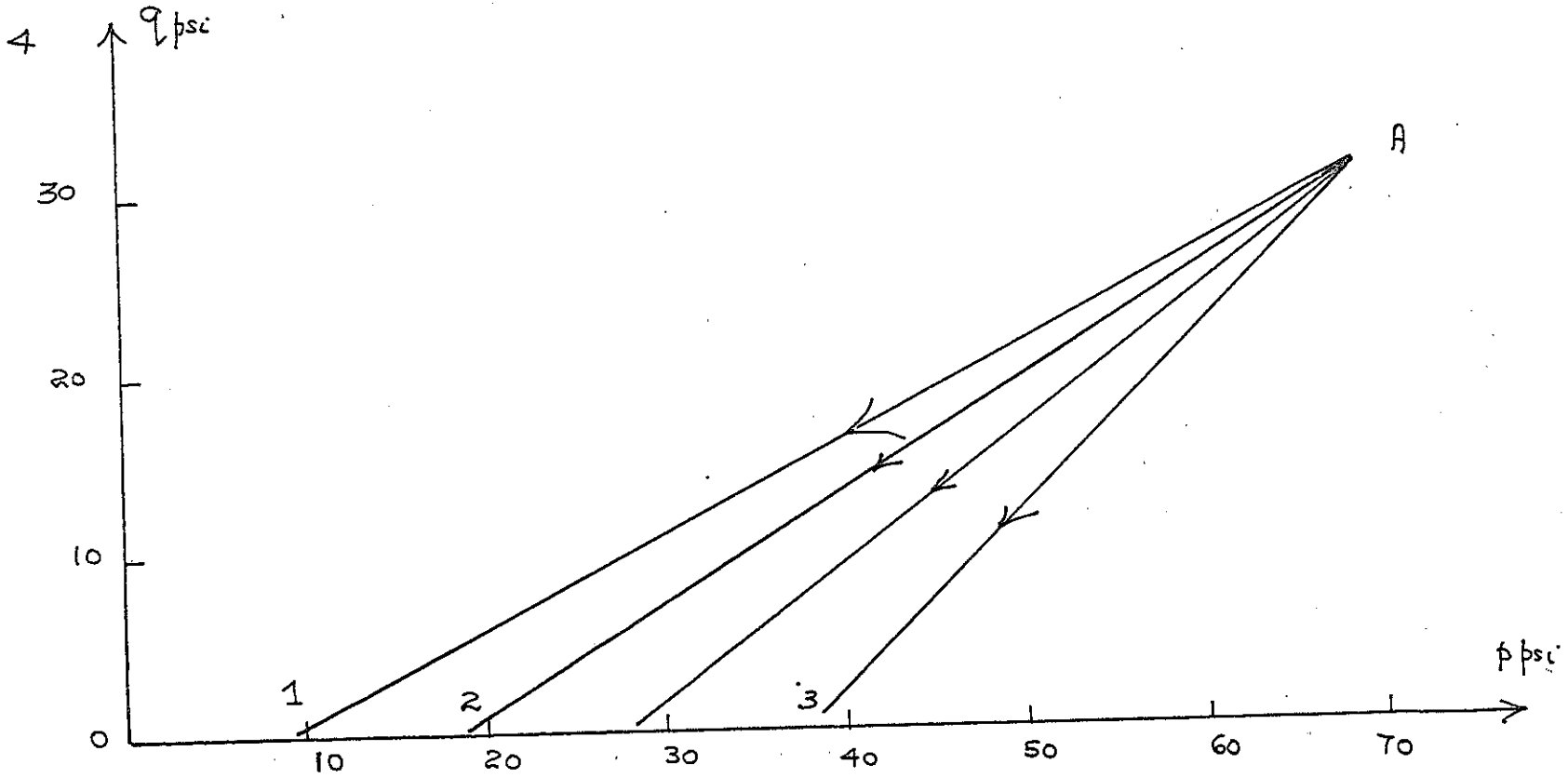


Fig. 7.40 (b). The stress path followed by specimen $T_{I9}$ during unloading from a stress ratio of $\eta = 0.47$

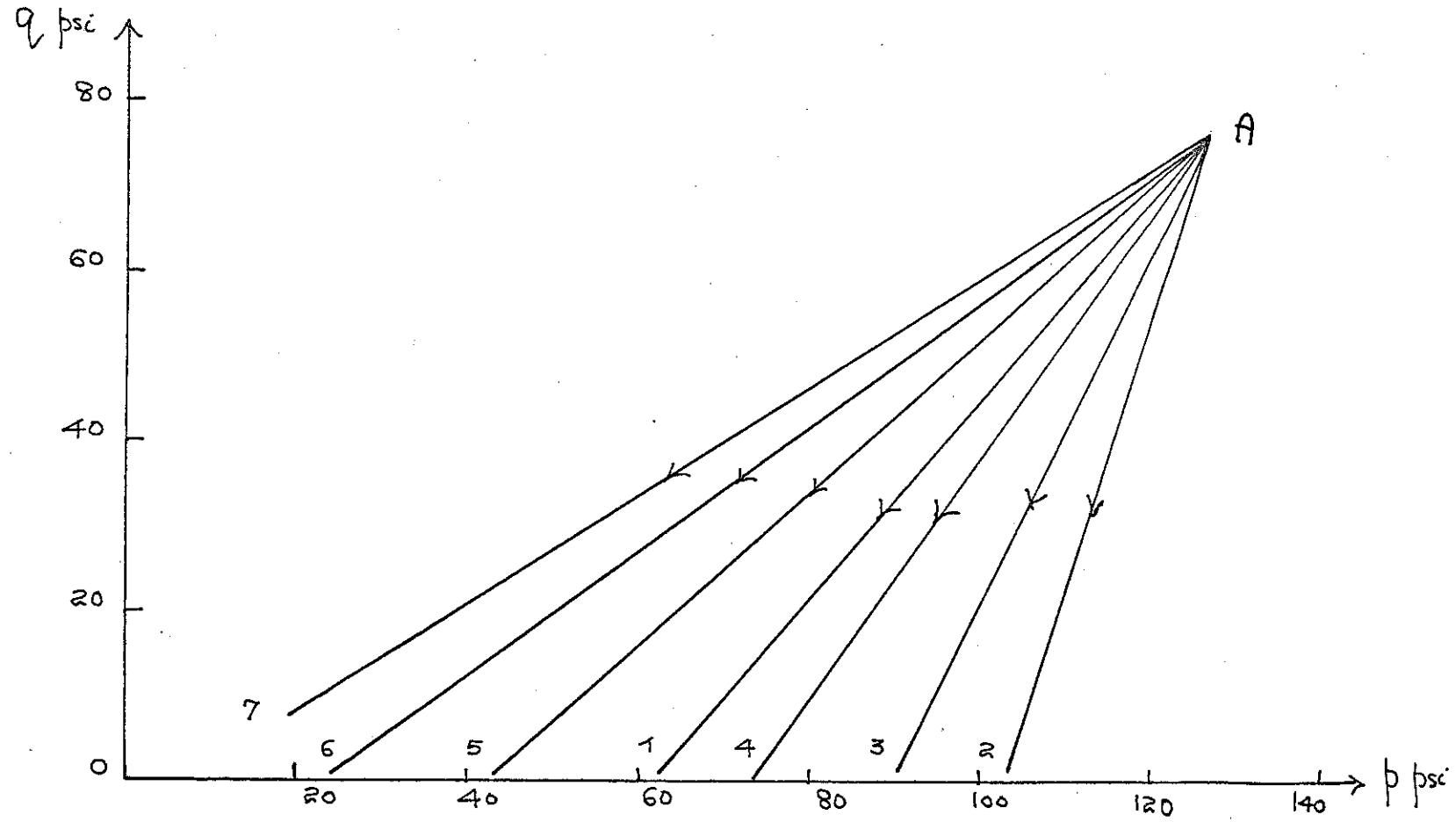


Fig. 7.40(c). The stress paths followed by specimen CB during unloading from a stress ratio of $\eta = 0.58$

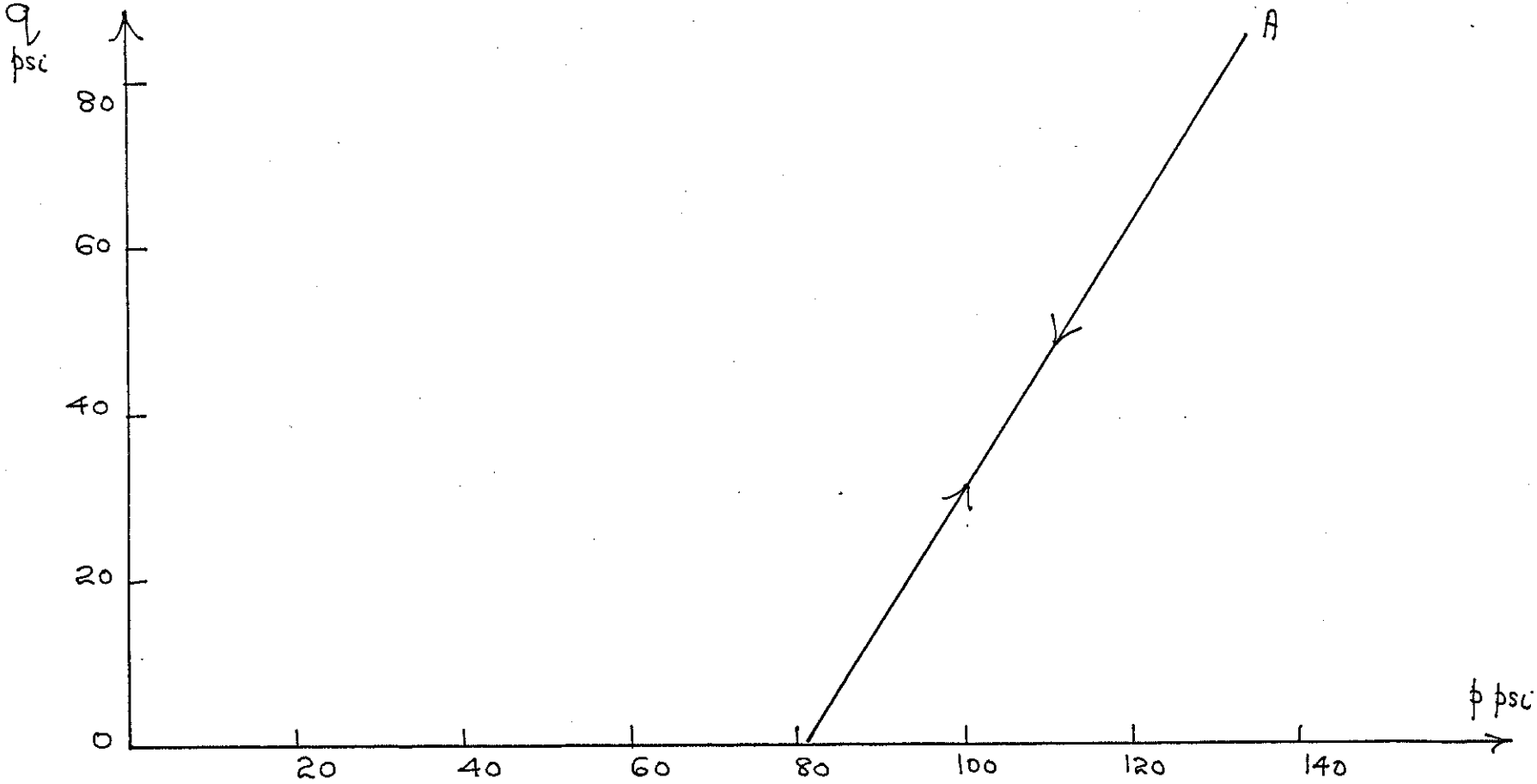


Fig. 7.40(d). The stress path followed by specimen BP during unloading from a stress ratio $\eta = 0.64$

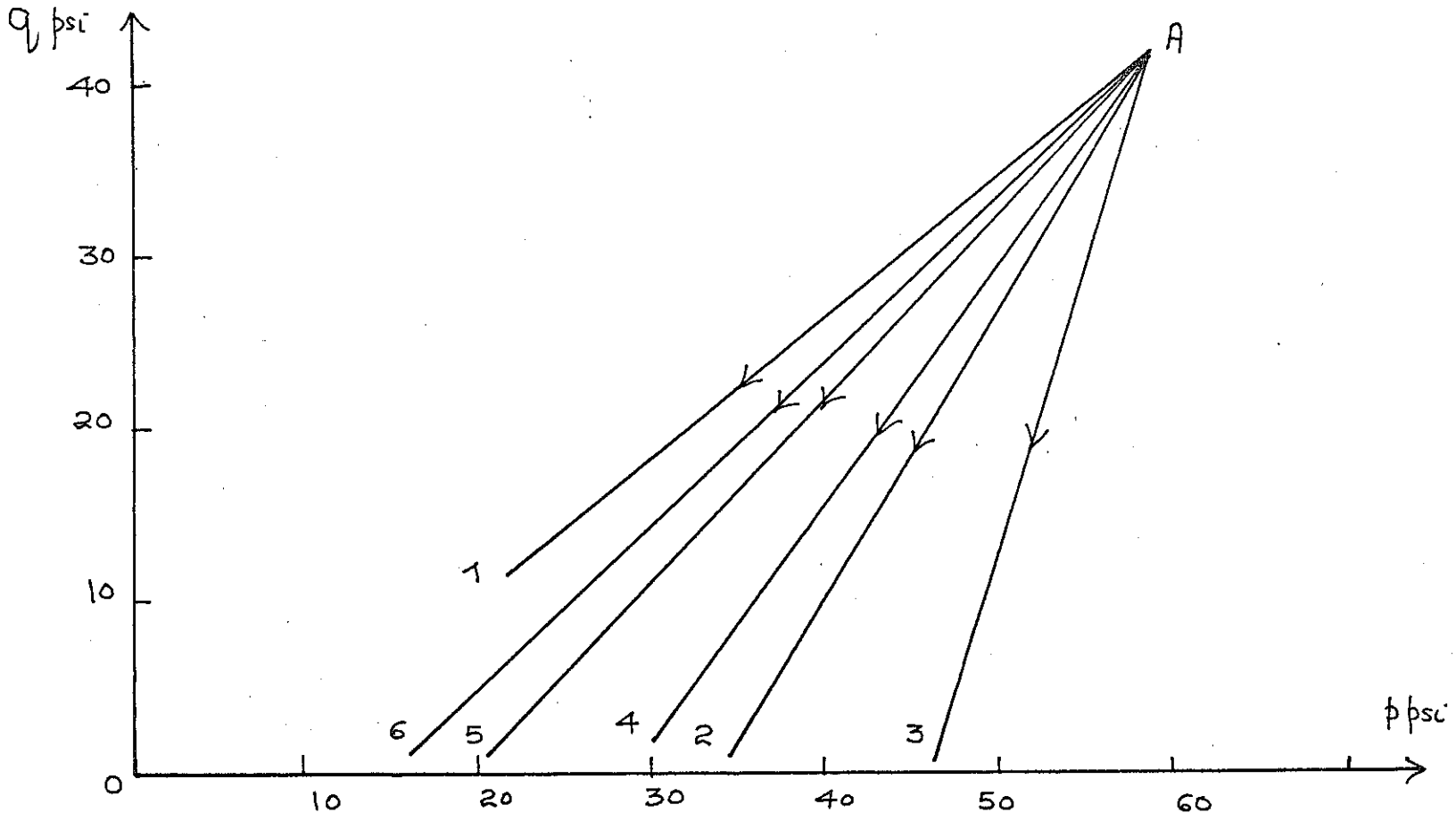


Fig. 7·40(e). The stress paths followed by specimen $T_{I6}$ during unloading from a stress ratio of $\eta = \overset{0.75}{\wedge}$

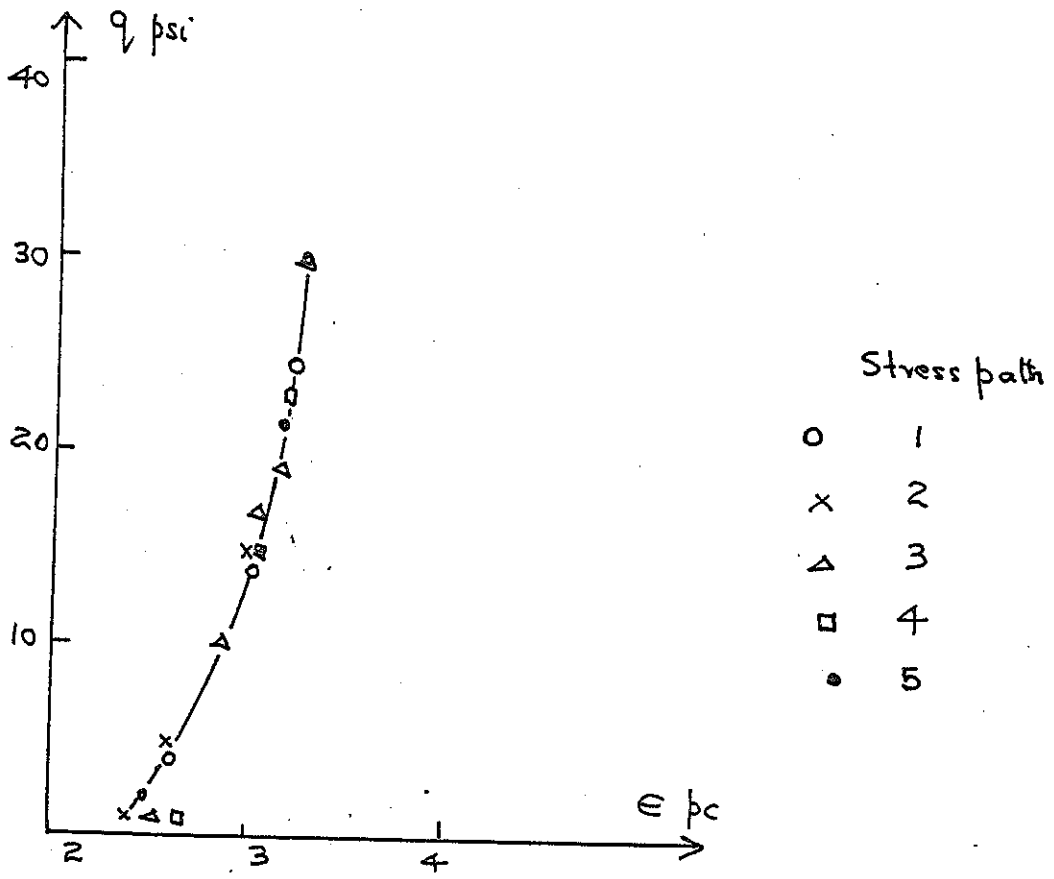


Fig. 7.4I (a). The $(q, \epsilon)$ characteristics of specimen $T_{20}$ during unloading from a stress ratio of $\eta = 0.34$

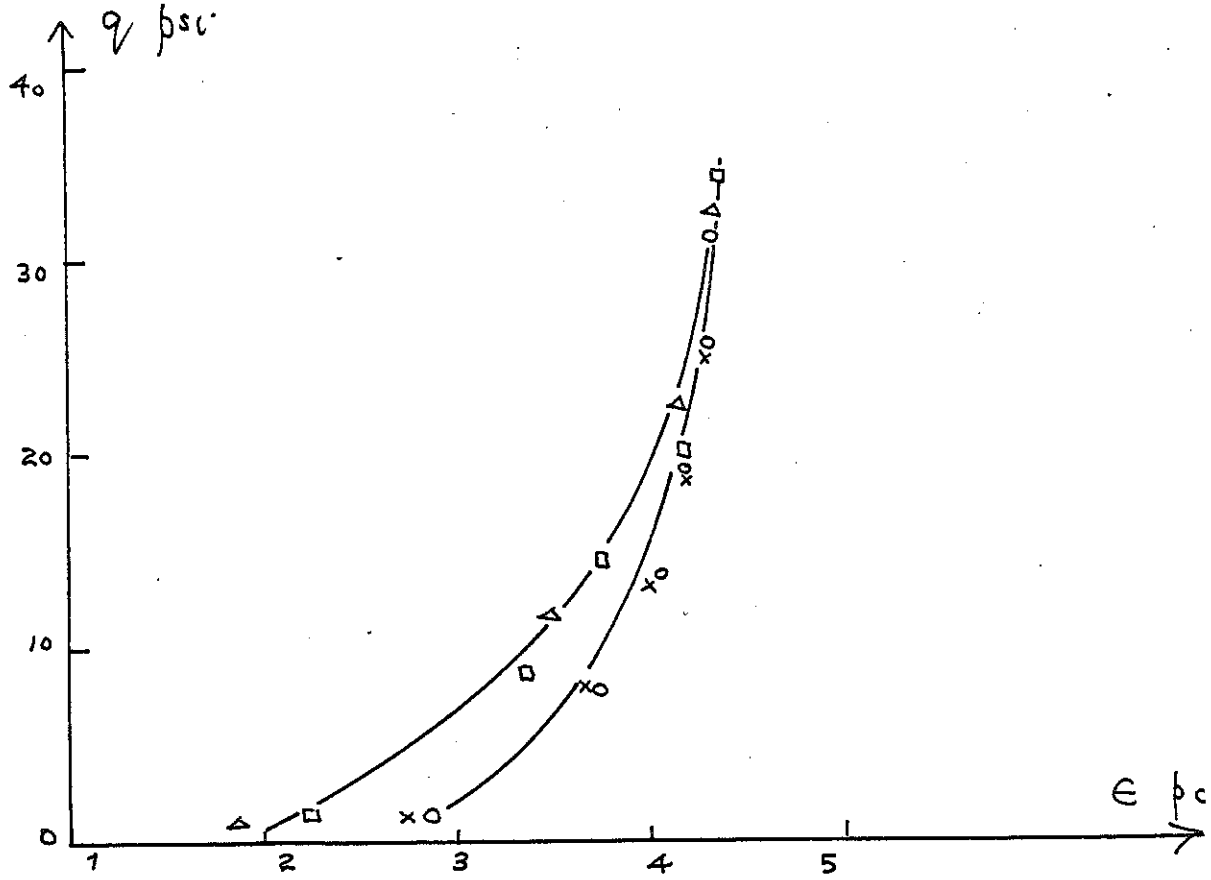


Fig. 7.4I (b). The ( q, $\epsilon$ ) characteristics of specimen $T_{I9}$ during unloading from a stress ratio of $\eta \neq 0.47$

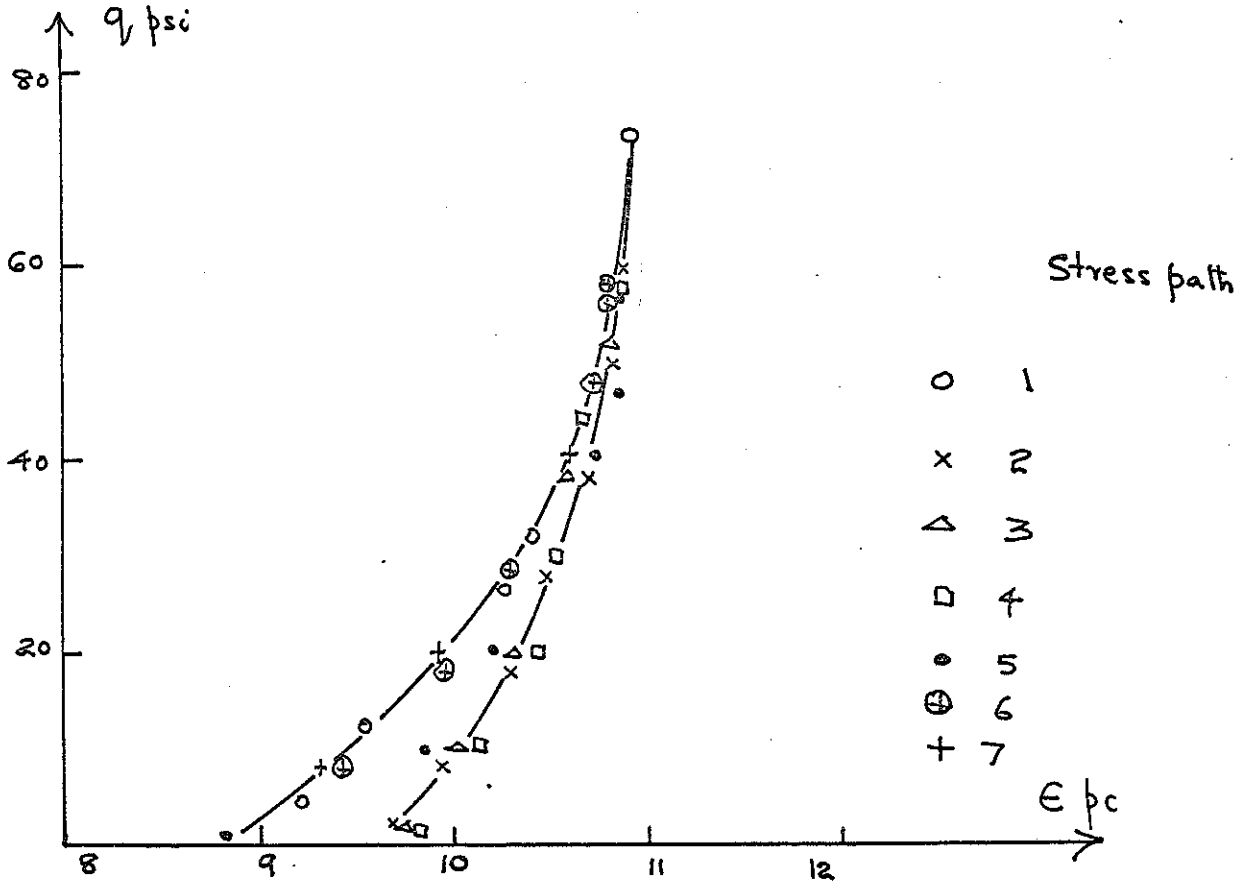


Fig. 7.4I (c). The ($q$, $\epsilon$) characteristics of specimen CB during unloading from a stress ratio of $\eta = 0.58$

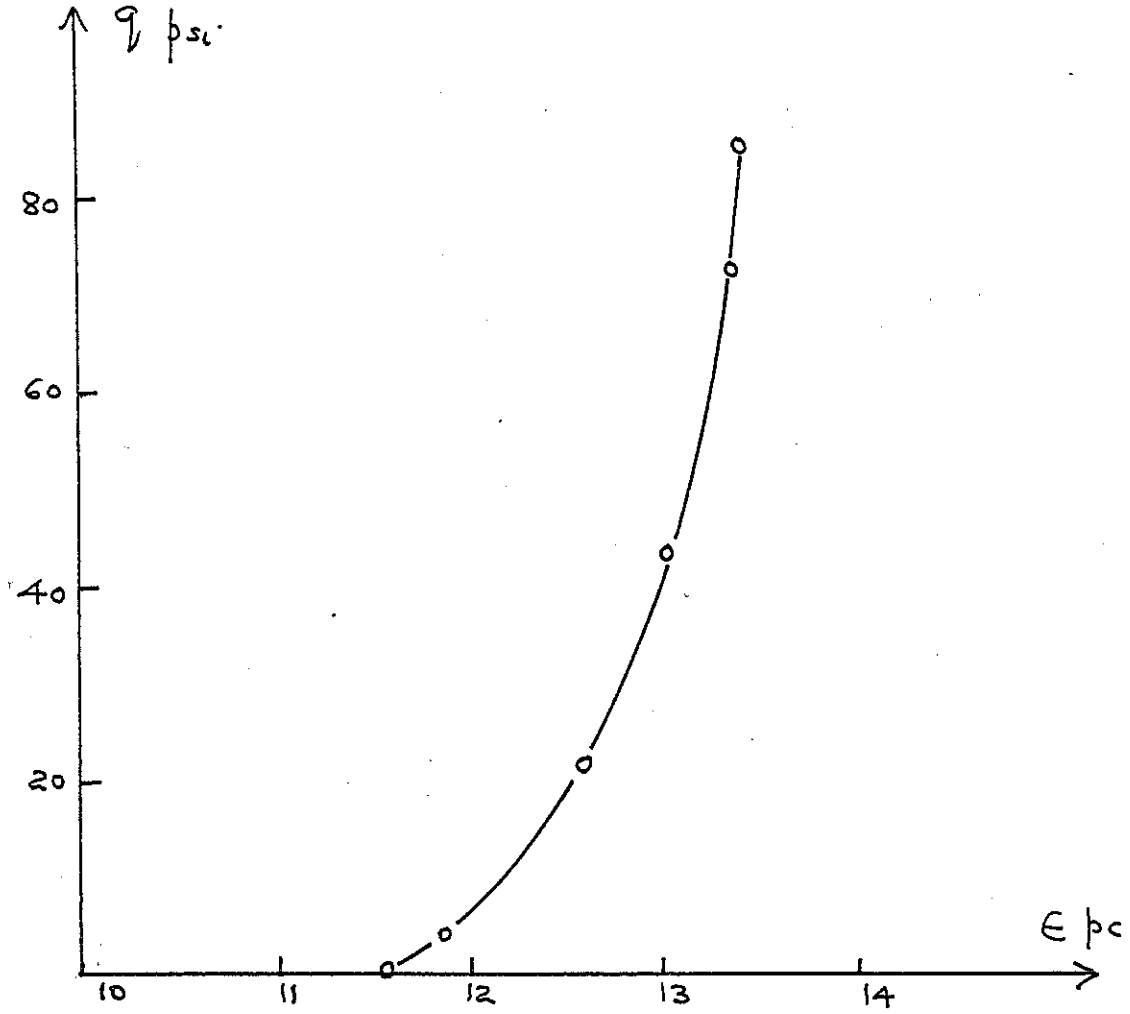


Fig. 7.4I (d). The $(q, \epsilon)$ characteristics of specimen BP during unloading from a stress ratio of $\eta = 0.64$

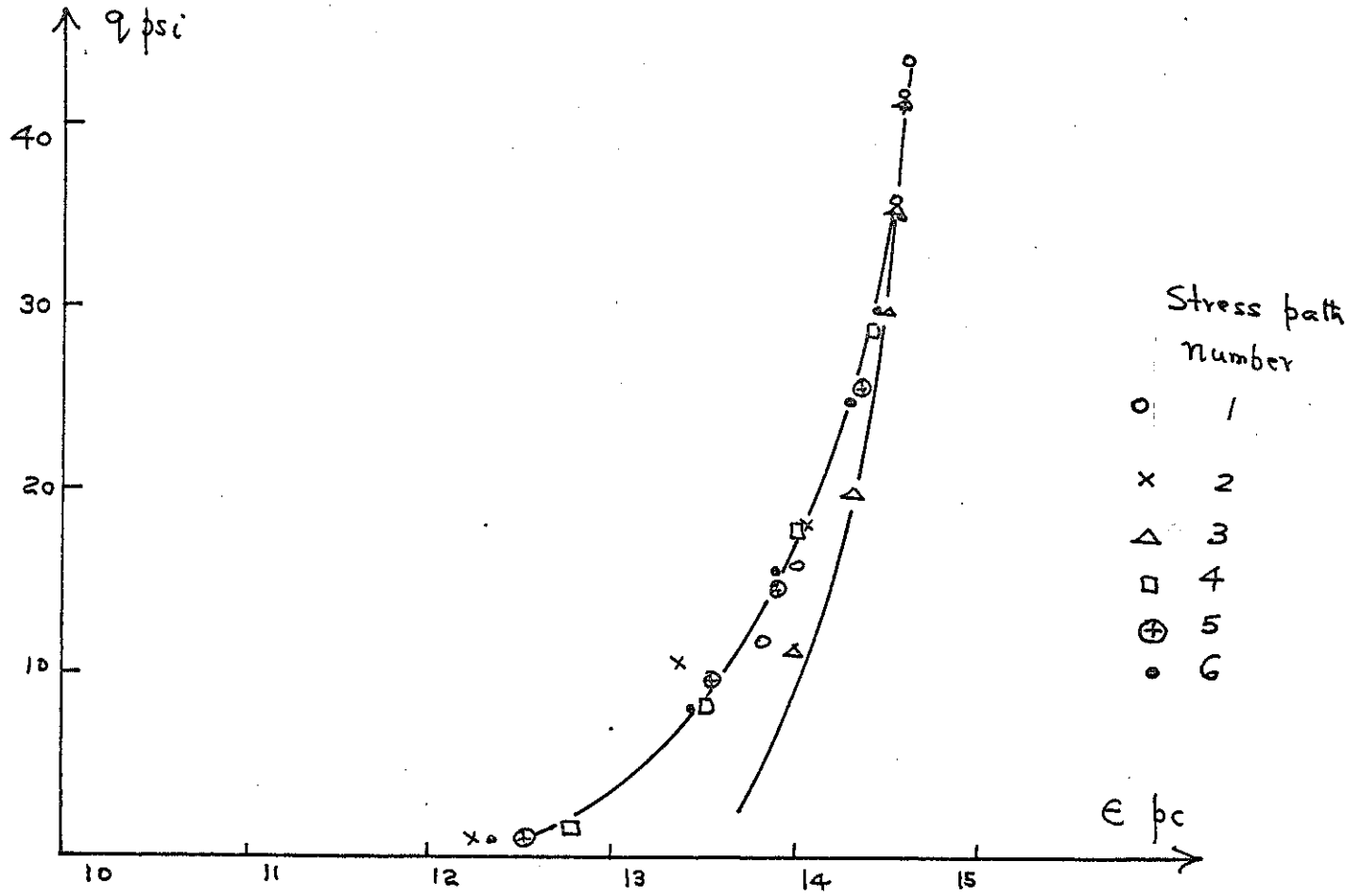


Fig. 7.4I (e). The $(q, \epsilon)$ characteristics of specimen $T_{I6}$ during unloading along stress paths indicated in Fig, 7.40 (e) from a stress ratio of $\eta = 0.74$

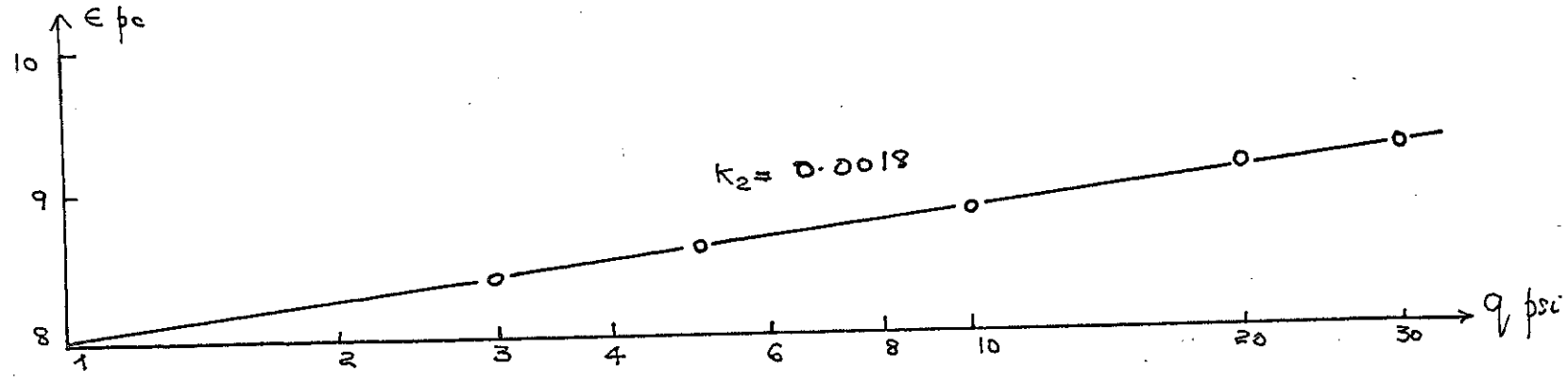


(a) From stress ratio $\eta = 0.34$

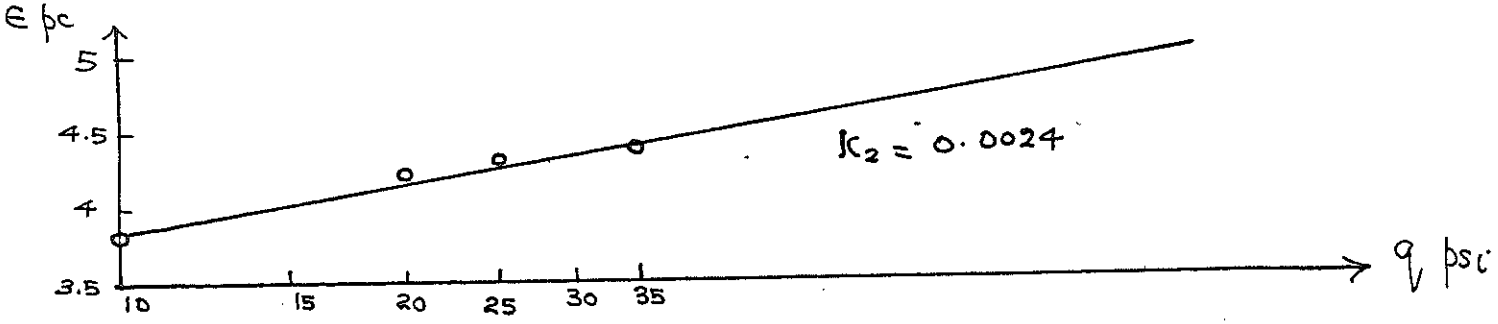


(b) From stress ratio $\eta = 0.47$

(See over-leaf )

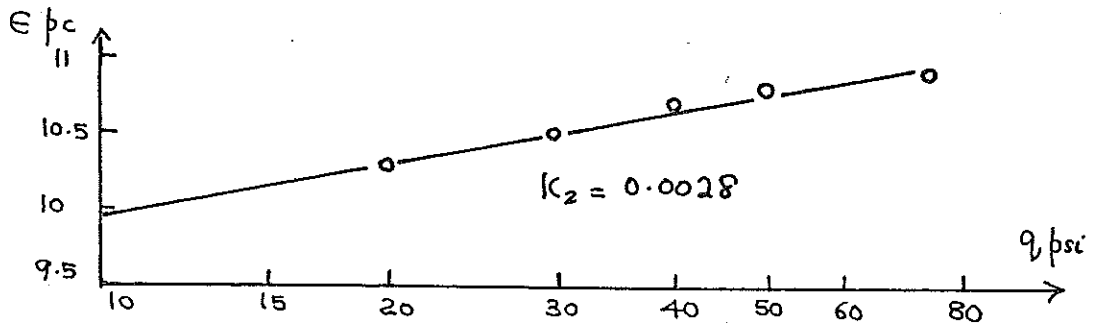


(c) From stress ratio $\eta = 0.577$

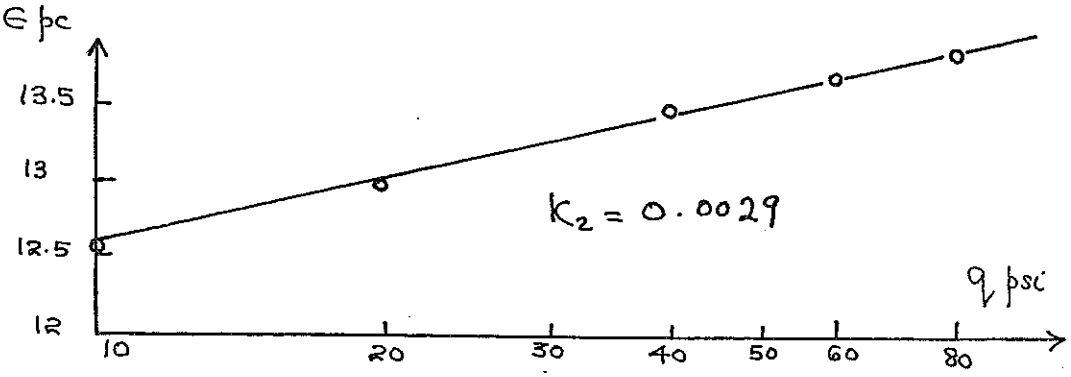


(d) From stress ratio $\eta = 0.64$

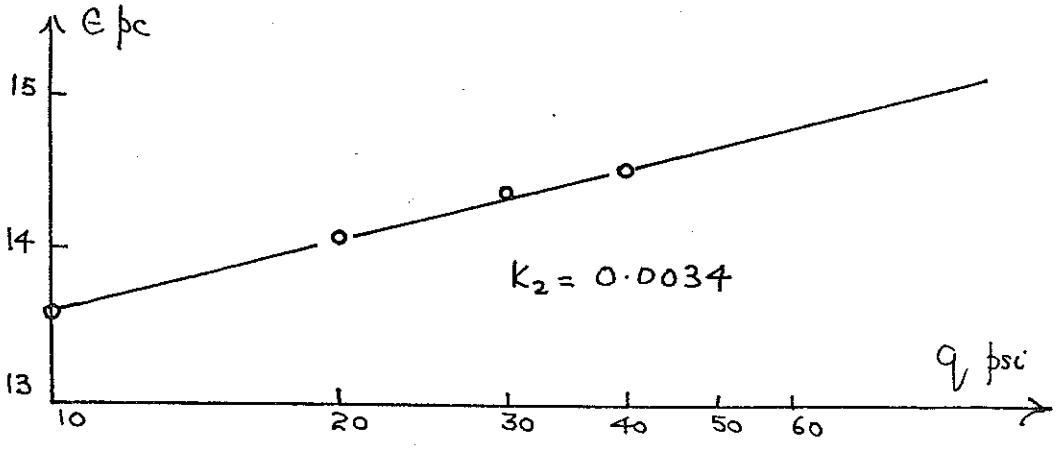


(e) From stress ratio $\eta = 0.74$

Fig. 7.42. The ( $\epsilon$ , $\log q$) characteristics of specimens unloaded from five different stress ratios.

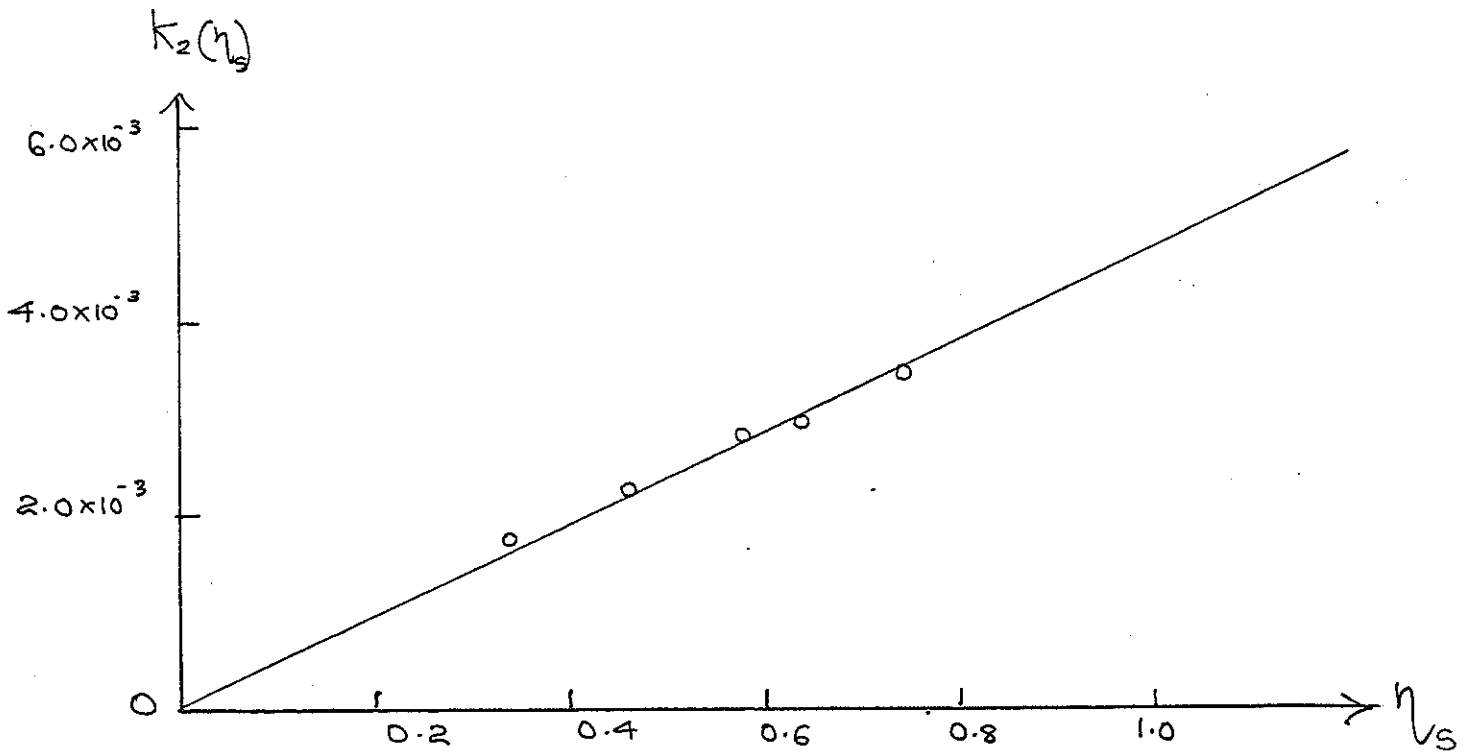


Fig. 7.43. The variation of $k_2(\eta_s)$ with $\eta_s$

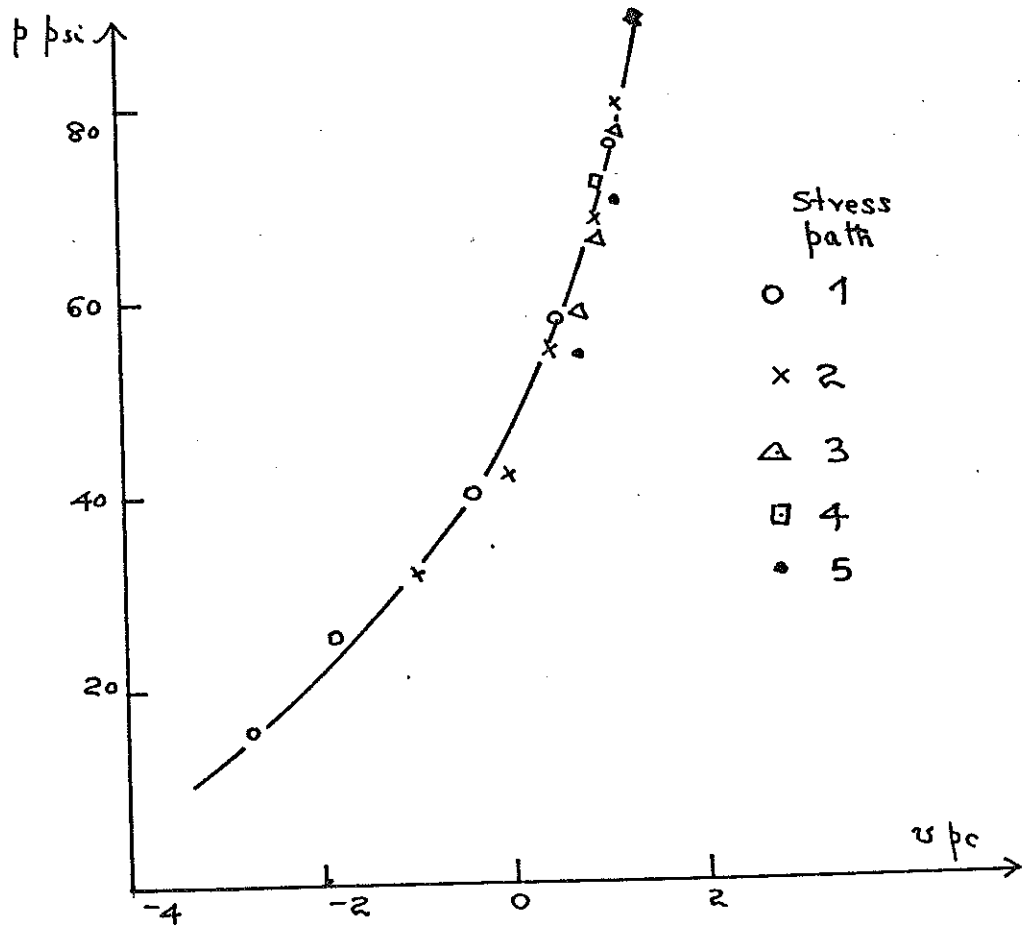


Fig. 7.44 (a). The ($p$, $v$) characteristic of specimen $T_{20}$ during unloading from a stress ratio of 0·34

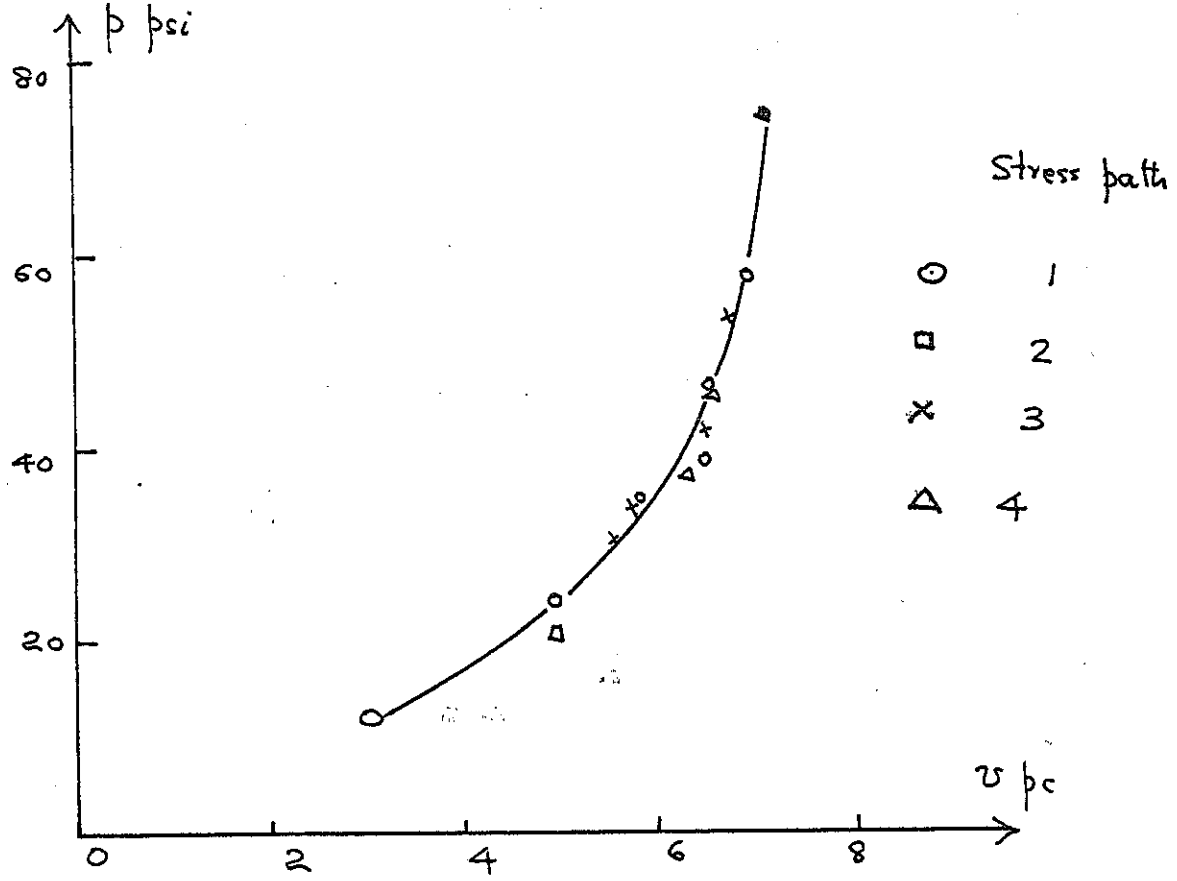


Fig. 7.44 (b). The ($p$, $v$) characteristic of specimen $T_{I9}$ during unloading from a stress ratio of 0.47

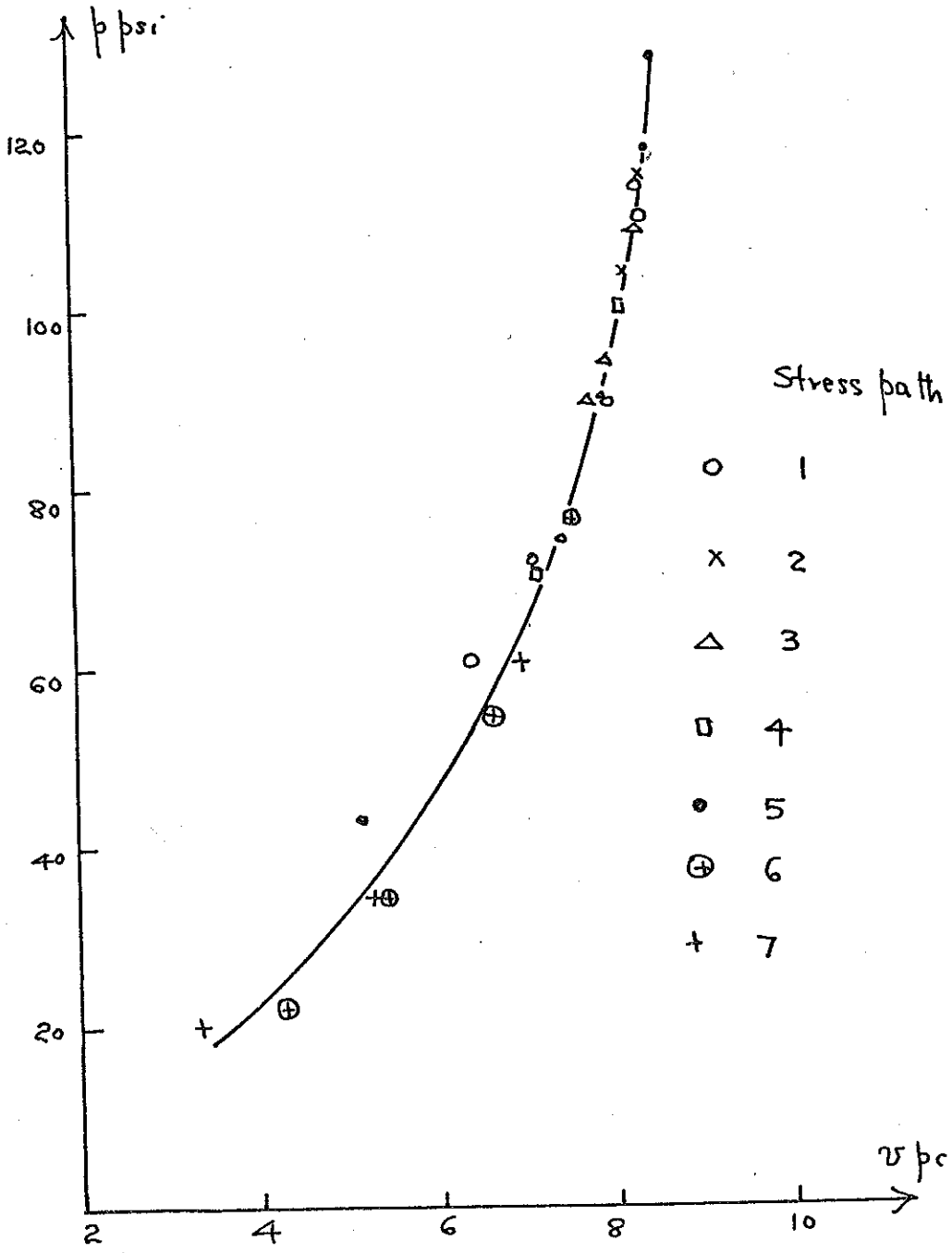


Fig. 7.44 (c). The ($p$, $v$) characteristic of specimen CB during unloading from stress ratio $\eta = 0.58$

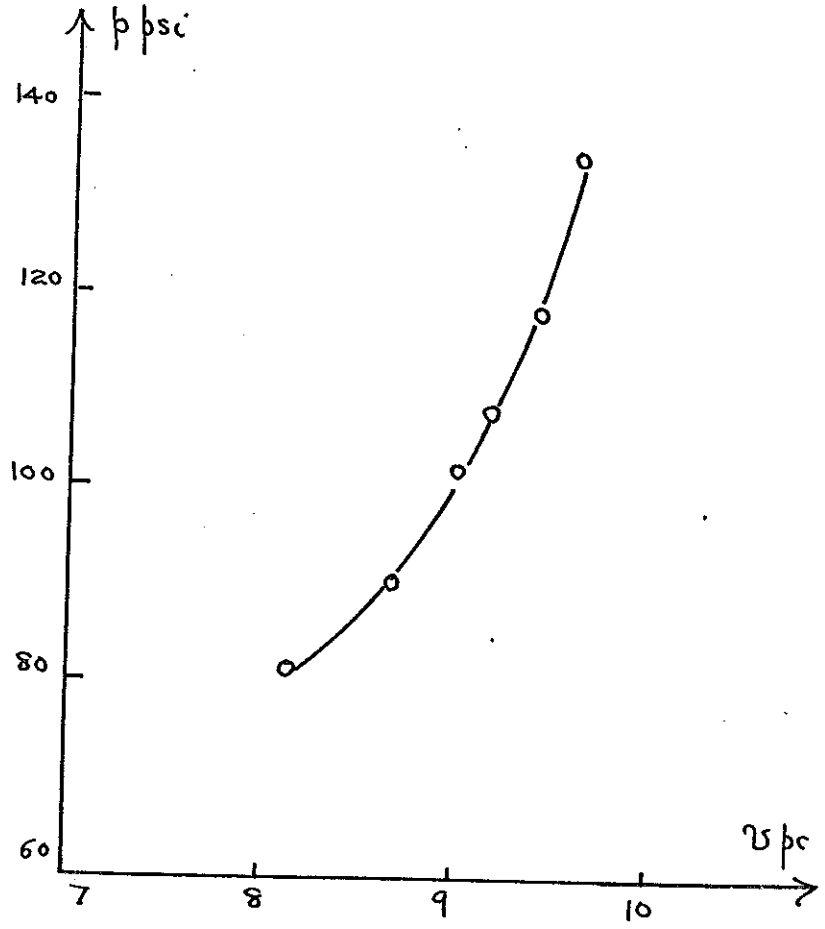


Fig. 7.44 (d). The ( p, $v$ ) characteristic of specimen BP during unloading from a stress ratio of $\eta = 0.64$

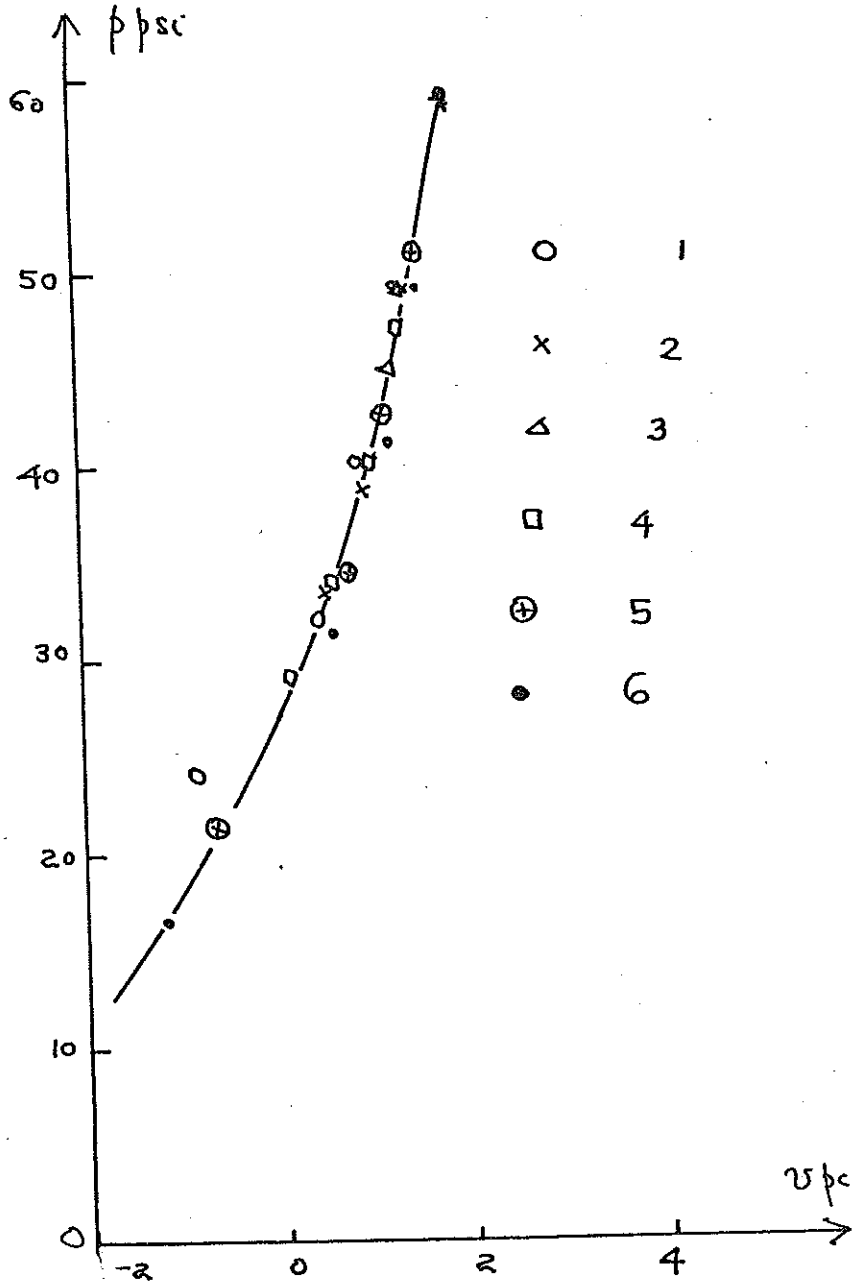


Fig. 7.44 (e). The ( $\phi$ , $v$ ) characteristic of specimen $T_{I6}$ during unloading from a stress ratio = 0.75

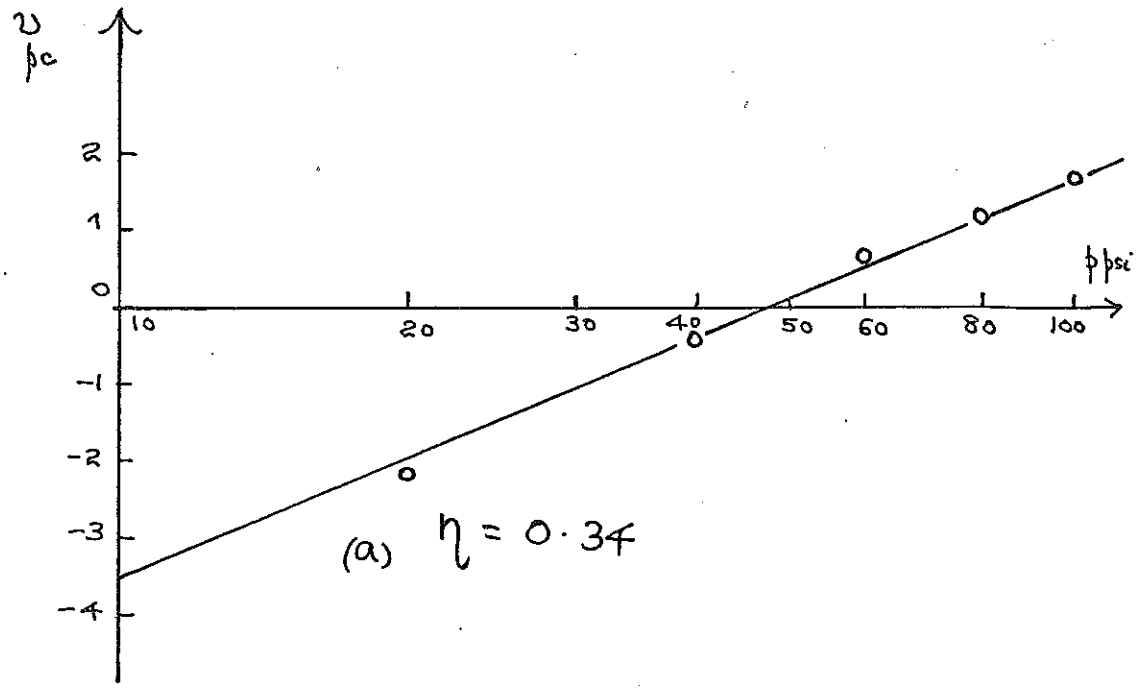


(a) $\eta = 0.34$

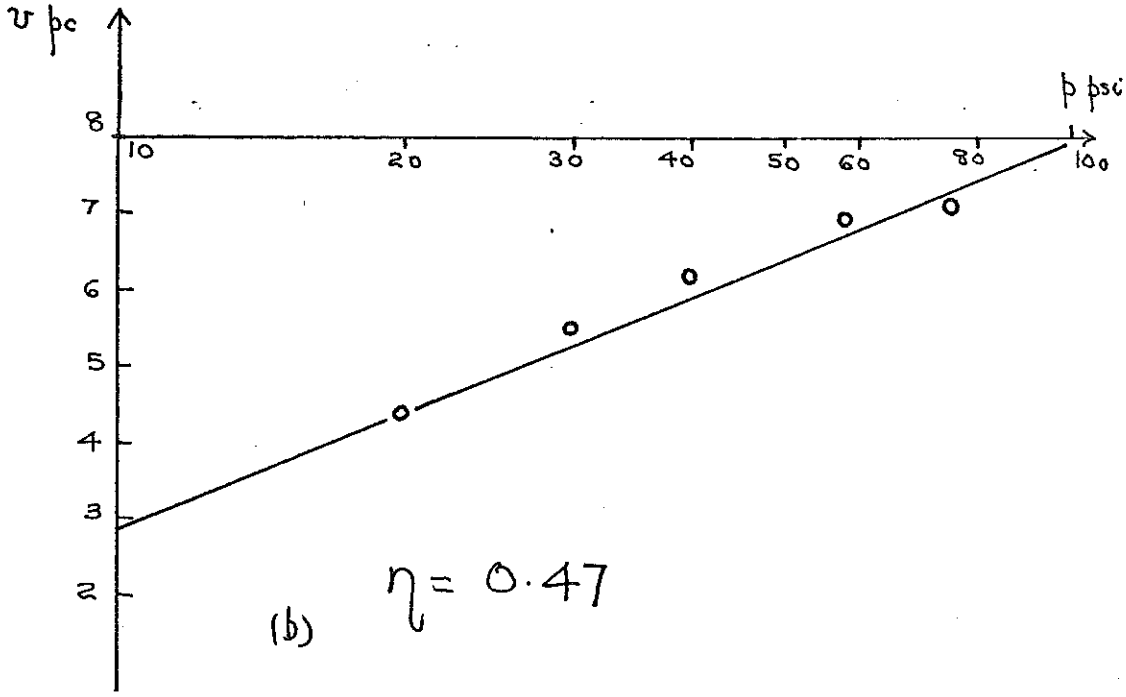


(b) $\eta = 0.47$

See overleaf

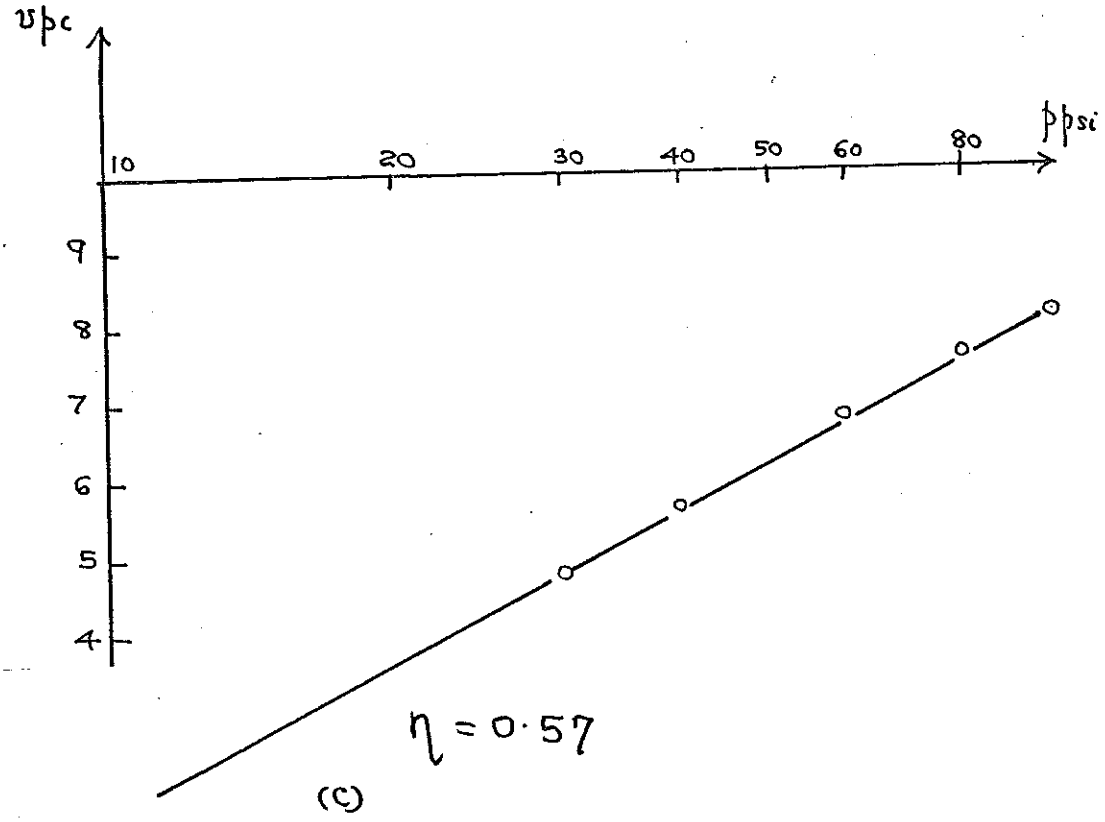


$\eta = 0.57$

(c)

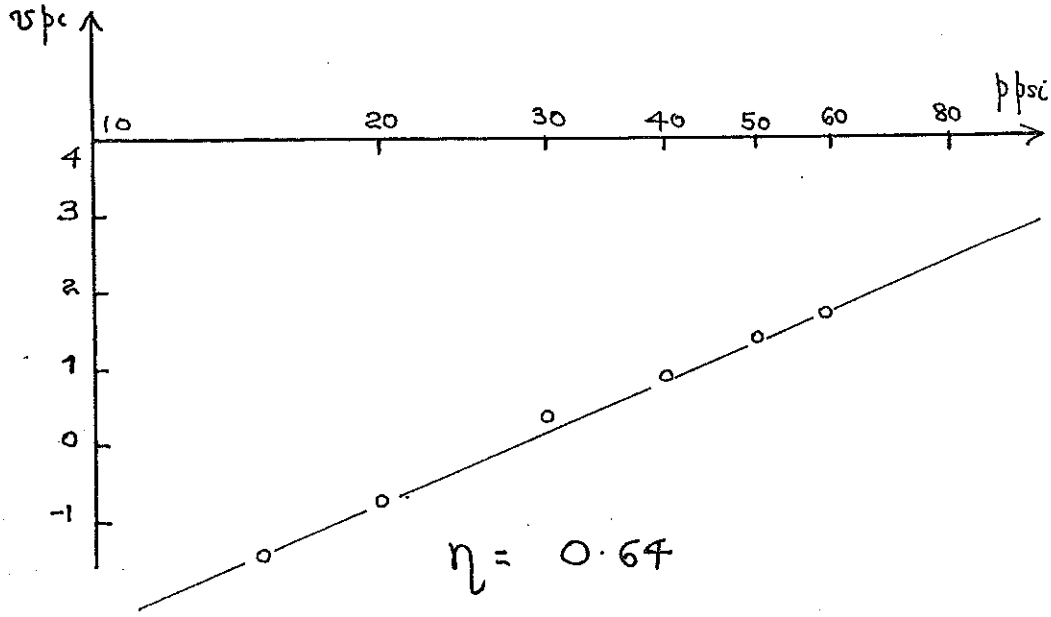


$\eta = 0.64$

(d)

See overleaf

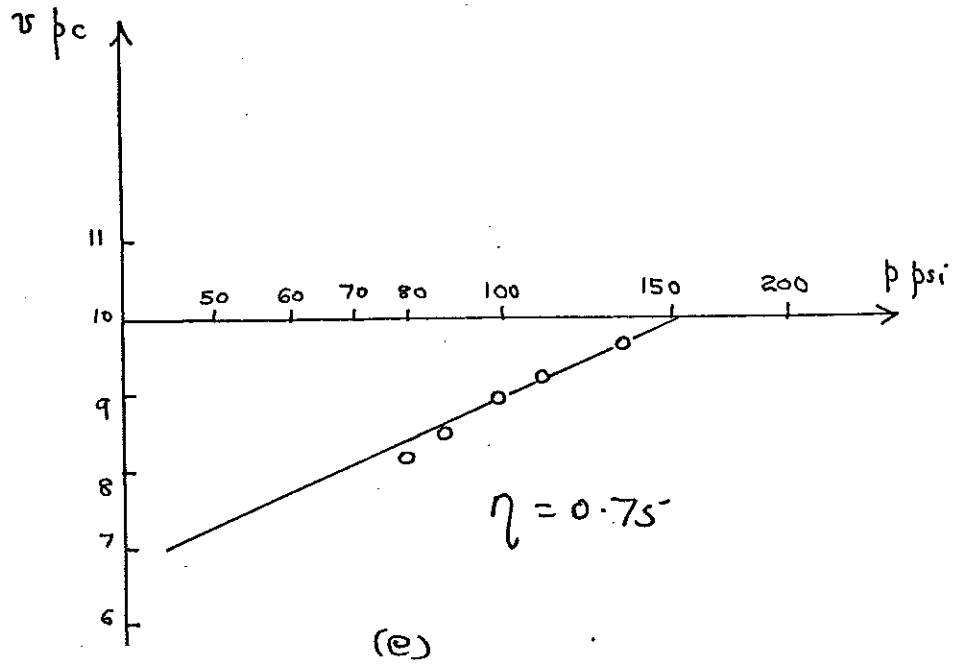


Fig. 7.45 (a-e) The ( $v$ , $\log p$ ) characteristics of specimens unloaded from stress ratios $\eta$ = 0·34, 0·47, 0·57, 0·64 and 0·75

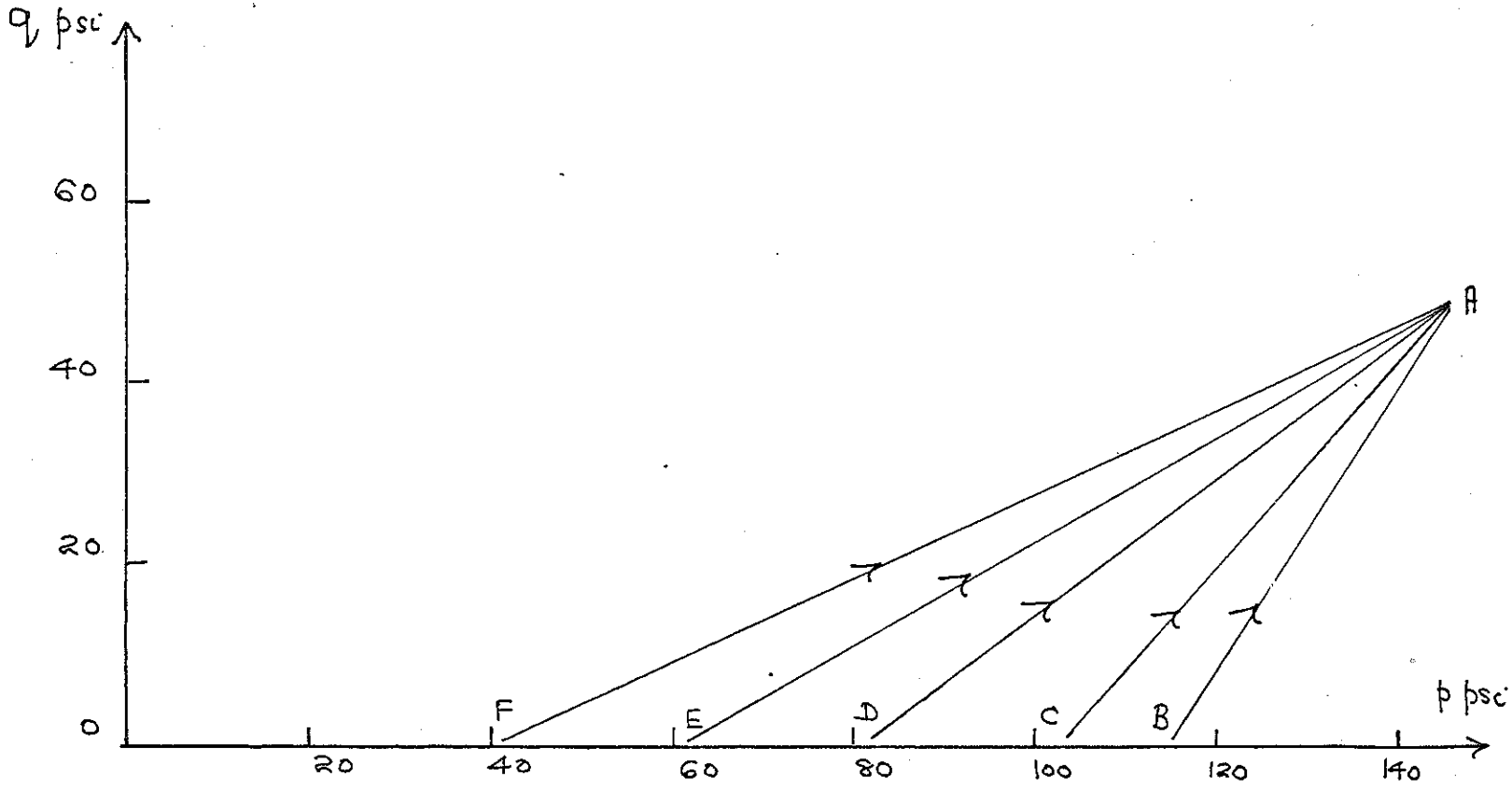


Fig. 7.46. The stress paths followed by specimen CG during reloading to stress ratio $\eta_s = 0.34$

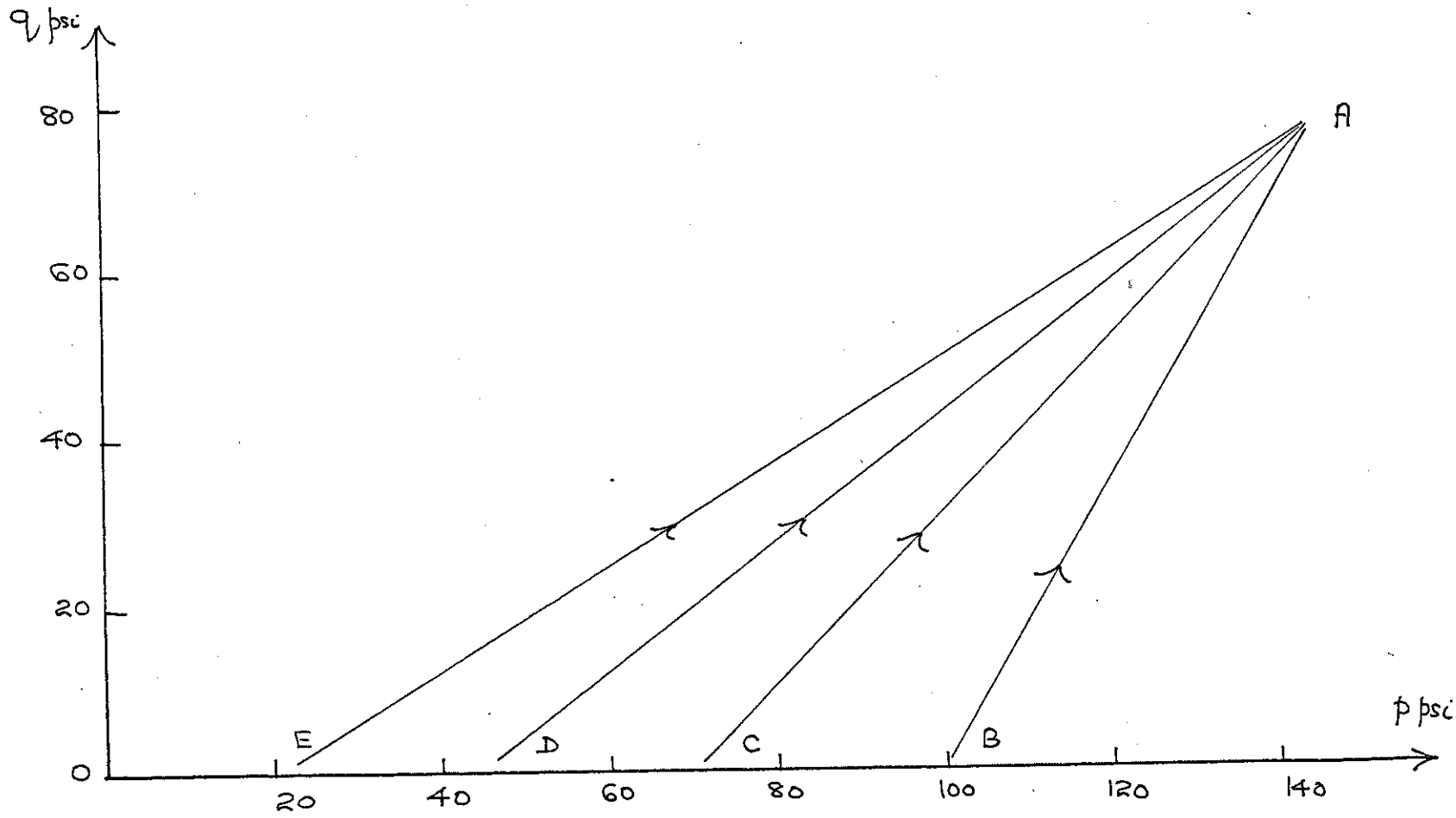


Fig. 7.47. The stress paths followed by specimen CG during reloading to stress ratio $\eta_s = 0.53$

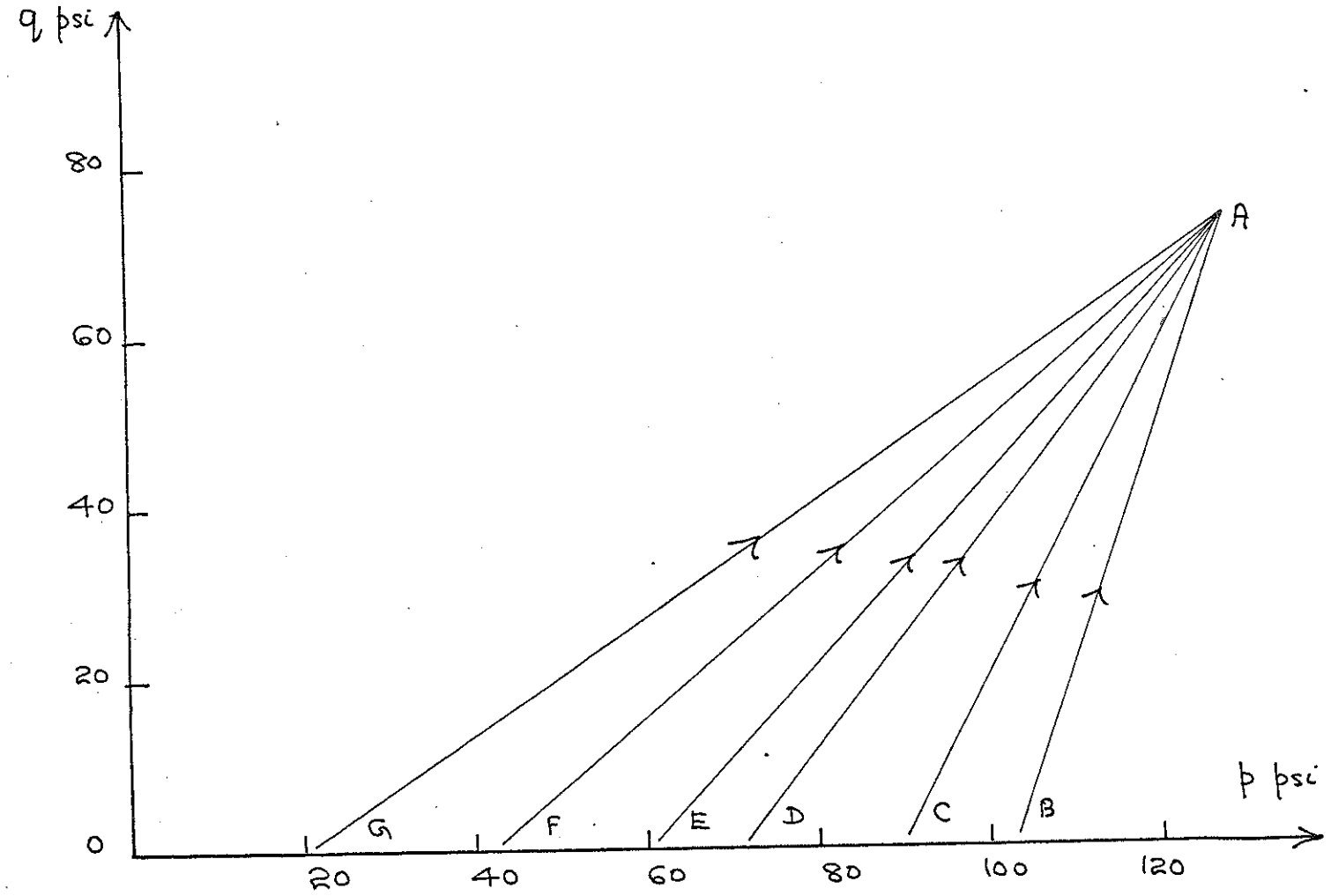


Fig. 7.48. The stress paths followed by specimen CB during reloading to stress ratio $\eta_s = 0.58$

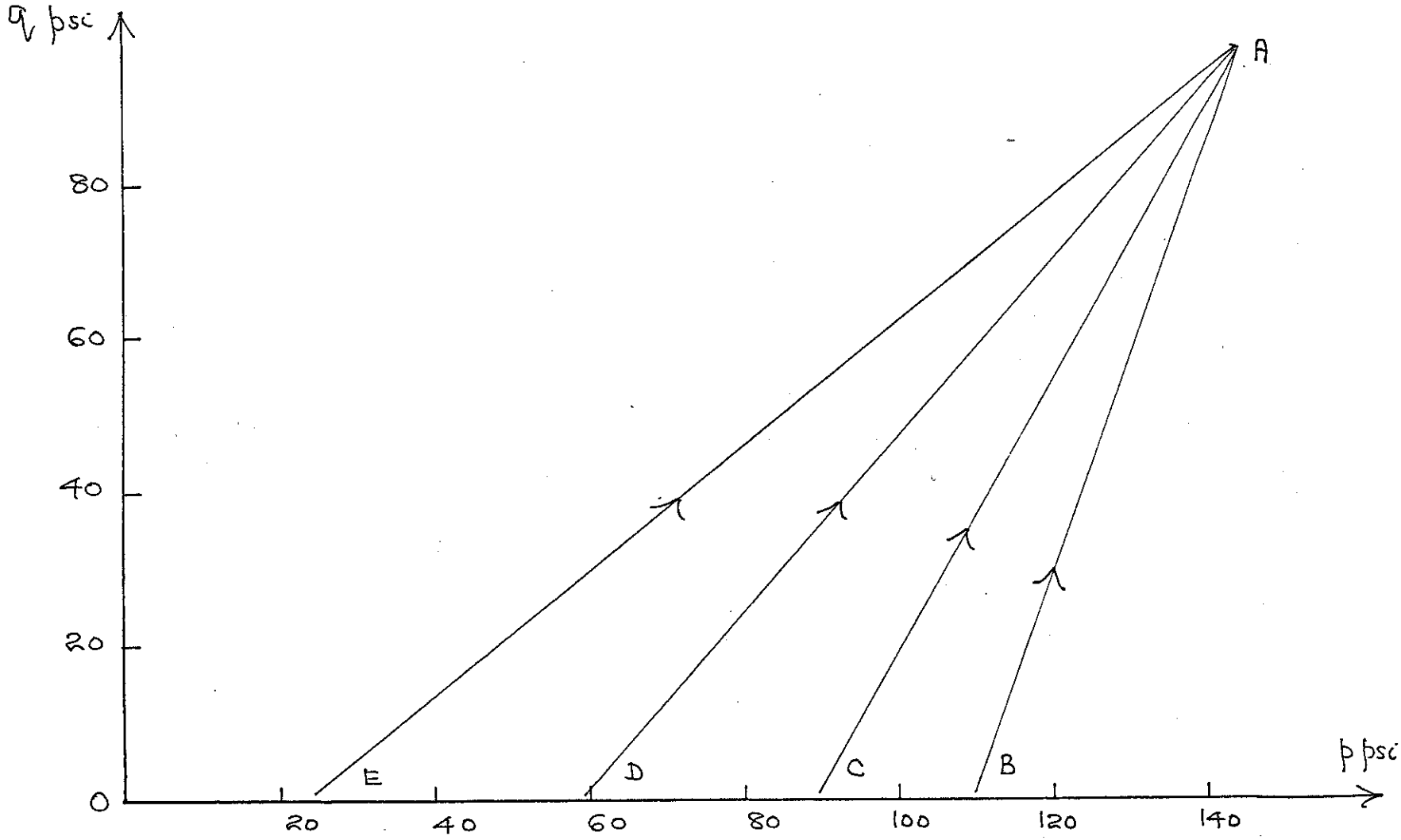


Fig. 7.49 The stress paths followed by specimen CG during reloading to stress ratio $\eta_s = 0.68$

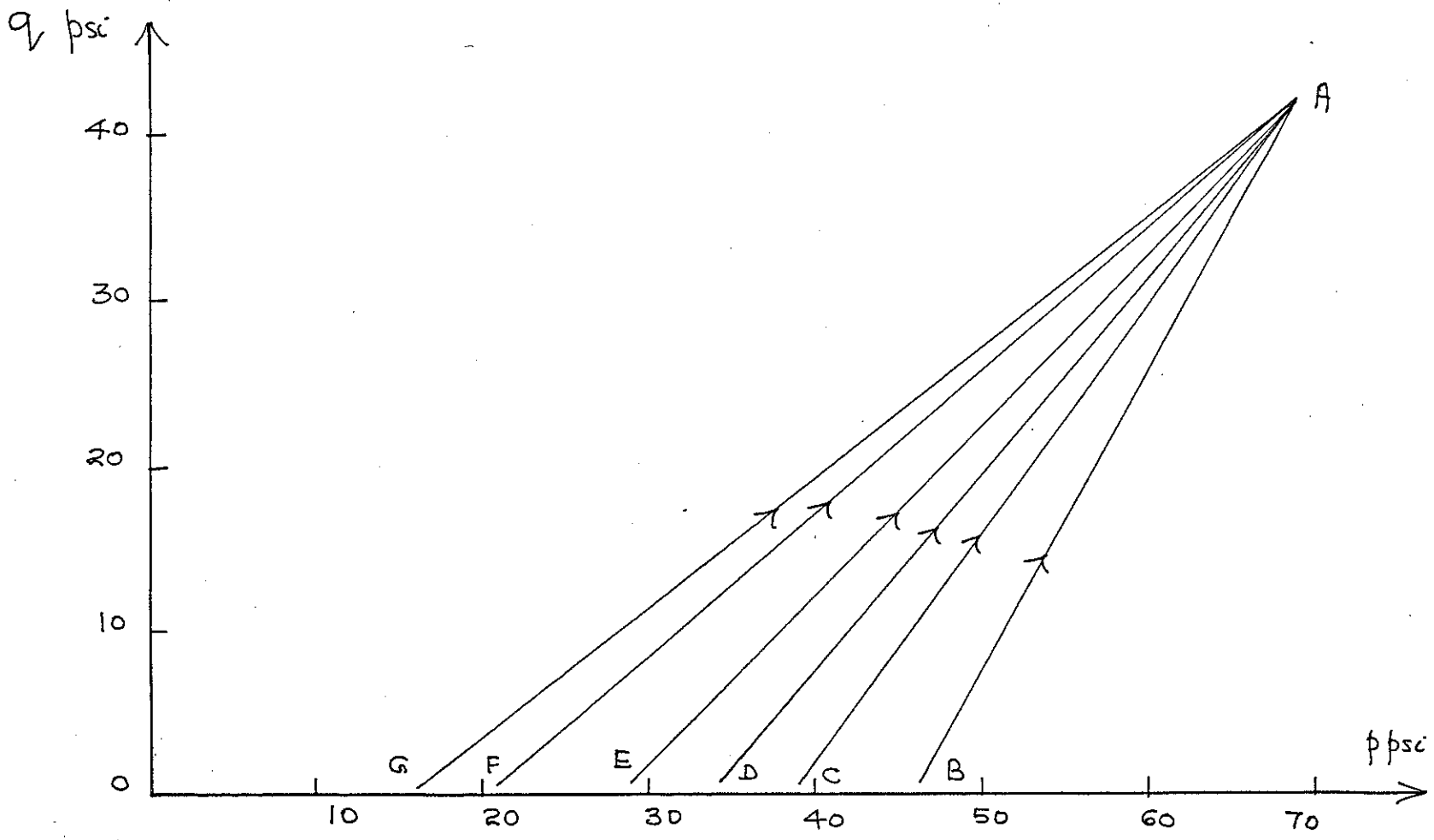


Fig. 7.50. The stress paths followed by specimen $T_{16}$ during reloading to stress ratio $\eta_s = 0.75$

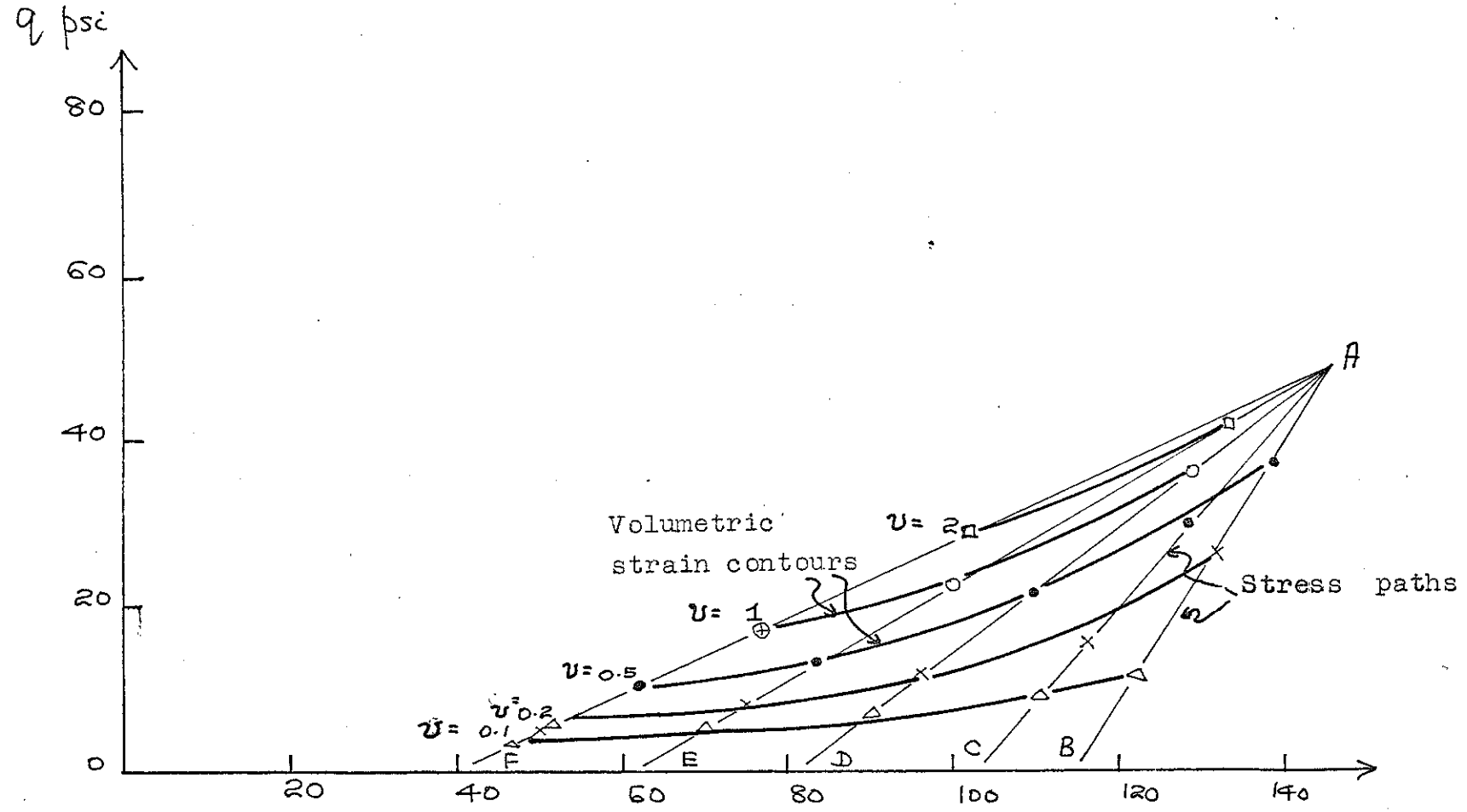


Fig. 7.51. Volumetric strain contours of specimen CG during reloading to stress ratio $\eta_s = 0.34$

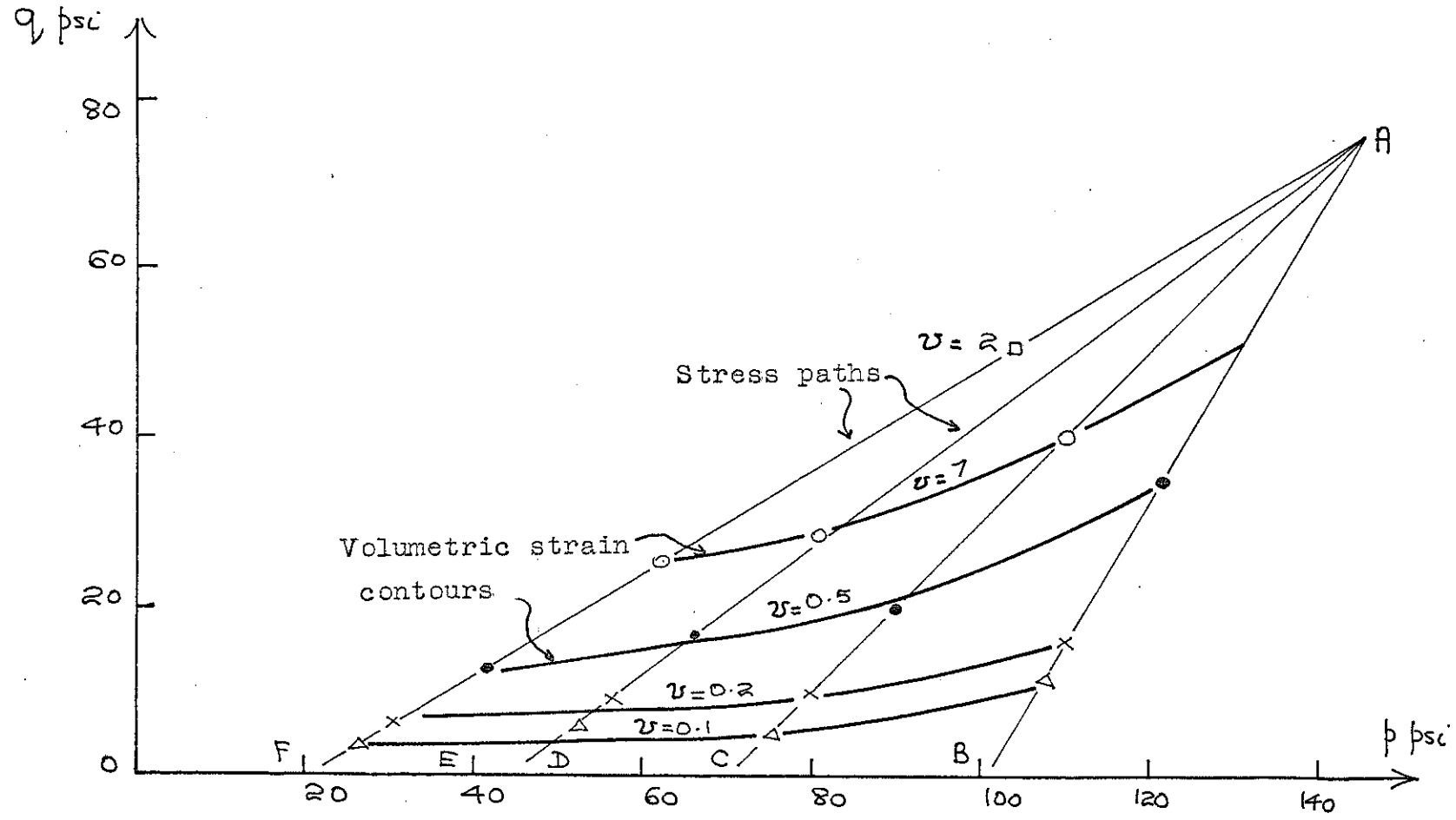


FIG. 7.52. Volumetric strain contours of specimen CG during reloading to stress ratio $\eta_s = 0.53$

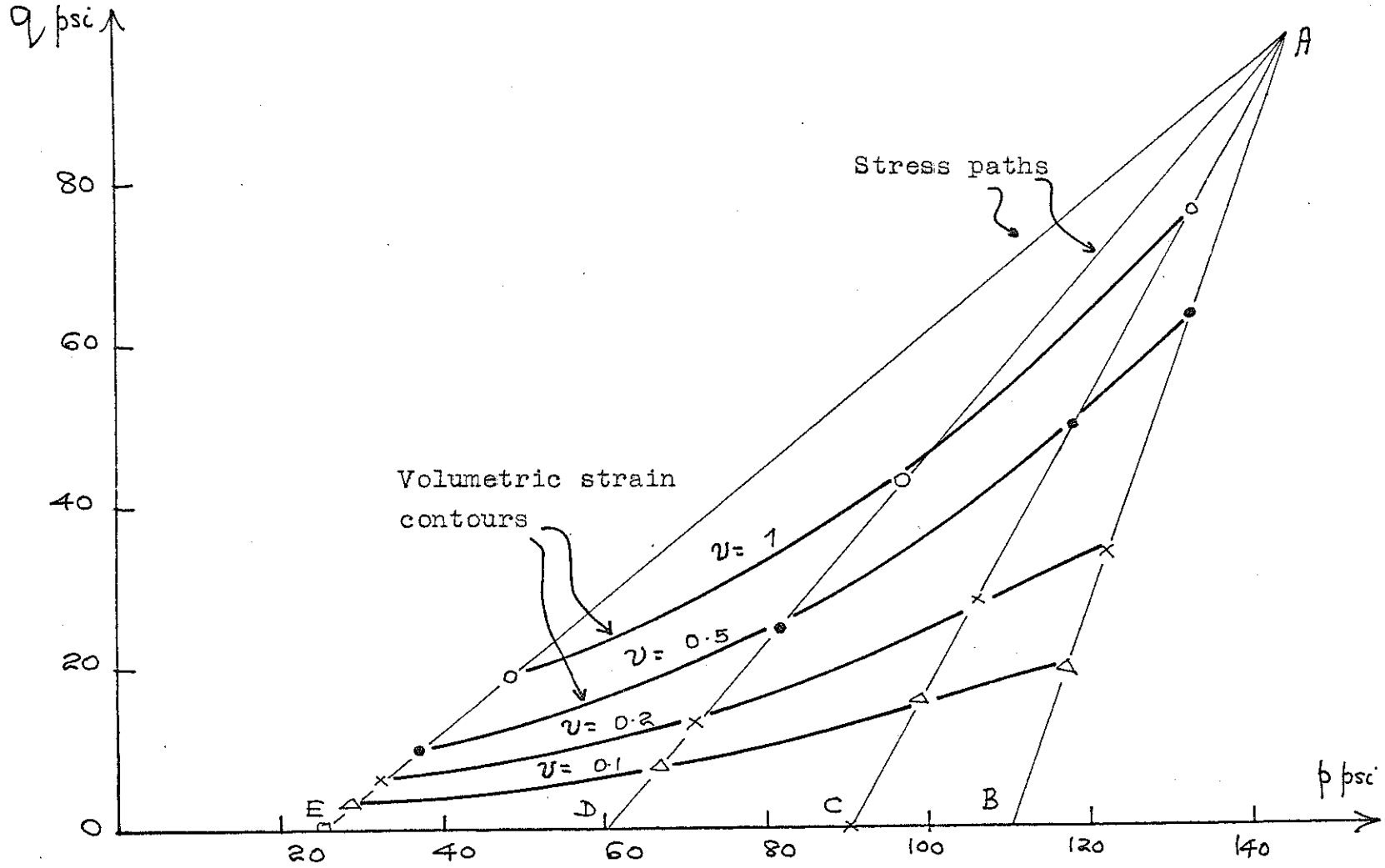


Fig. 7.53. Volumetric strain contours of specimen CG during reloading to stress ratio $\eta_s = 0.58$